

Electric Quadrupole Effects in Nuclear Magnetic Resonance in the Case of Large Nuclear Spin. The Nuclear-Magnetic-Resonance Spectrum of Solid Indium*

R. G. BARNES, D. J. GENIN, R. G. LECANDER, AND D. R. TORGESON

Institute for Atomic Research and Department of Physics, Iowa State University, Ames, Iowa

(Received 9 December 1965)

The nuclear-magnetic-resonance spectrum of In^{115} in polycrystalline indium (powder) reveals a number of unusual features stemming from the combination of large quadrupole interaction and large nuclear spin ($I = \frac{9}{2}$). The crossing of several Zeeman transitions, the occurrence of non-90° satellite lines, and the occurrence of forbidden transitions ($\Delta m = \pm 2$) have been verified experimentally, and the experimental results have been compared with a detailed theoretical calculation of the spectrum based on exact numerical diagonalization of the secular determinant. At room temperature, the isotropic and anisotropic Knight-shift tensor components have the values $K_{\text{iso}} = +(0.82 \pm 0.04)\%$ and $K_{\text{ax}} = -(0.14 \pm 0.04)\%$.

I. INTRODUCTION

THE nuclear-magnetic-resonance (NMR) spectrum of In^{115} in polycrystalline indium (powder) provides an opportunity to observe and investigate a number of unusual features not ordinarily encountered in the NMR spectra of solids. These features stem from the effects which the combination of large nuclear spin ($I = \frac{9}{2}$) and large electric quadrupole interaction have on the nuclear Zeeman levels. In addition to the typical resonance spectrum consisting of a set of $2I - 1$ "satellite" lines and a split central transition ($m = +\frac{1}{2} \leftrightarrow -\frac{1}{2}$), which is obtained when the quadrupole coupling is sufficiently strong to yield second order effects, three new features are observed in the indium spectrum:

1 The high-field side of the split central transition crosses several of the satellite lines on the high-field side of the spectrum.

2 "Extra" satellite lines appear which are due to second and higher order effects on the satellites in a manner corresponding to the splitting of the central transition.

3 At moderately low field strengths, lines of the $\Delta m = \pm 2$ (forbidden) spectrum appear within the region of the $\Delta m = \pm 1$ (allowed) spectrum.

These observations in the case of indium demonstrate that for a metallic material, the presence of a large electric quadrupole interaction need not prevent the determination of the experimental parameters—quadrupole coupling and magnetic shift tensor components—using only a polycrystalline (powder) sample.¹ The NMR spectra of a number of other noncubic metals have been found to exhibit second-order quadrupole complications within the range of resonance frequencies typically studied. These include scandium,² magnesium,³ technetium,⁴ and bismuth⁵; but among these only the case

of bismuth compares with that of indium in terms of the relative magnitude of the quadrupole coupling and Zeeman energy. As has been previously emphasized,^{1,6} the significant comparison of these energies takes the form of the ratio, $\alpha = \nu_0/\nu_Q$, of the Zeeman frequency ν_0 to the lowest pure quadrupole frequency, ν_Q . Roughly speaking, second order effects of the quadrupole coupling become important when this ratio has the value 10, and third order effects begin to arise when this ratio equals 5 for the case of spin $\frac{9}{2}$. For smaller spin values these conditions are less stringent. In the case of indium, we have investigated the NMR spectrum over a field and frequency region extending from about $\alpha = 3$ to $\alpha = 20$.

The principal subject of the present paper is the comparison of the experimental NMR spectrum of In^{115} in polycrystalline indium metal (powder) at room temperature with a detailed theoretical calculation of that spectrum. The new features discussed above form a part of this spectrum. In addition, the present study confirms the conclusions reached on the basis of a perturbation-theory analysis of the central transition of this spectrum,¹ and shows that that type of analysis is satisfactory for the elucidation of the experimental resonance parameters, i.e., the quadrupole coupling and the isotropic and anisotropic Knight shifts.

In the following we shall first explain the origins of the new spectral features observed and then show and discuss the comparison of the experimental spectrum with the calculated one.

II. PERTURBATION-THEORY TREATMENT

The origins of the new features of the NMR spectrum in a powder specimen, which arise from the combination of large nuclear spin and large quadrupole interaction, can be semiquantitatively understood on the basis of perturbation theory even though a complete discussion of the indium spectrum on this basis is not worthwhile. Volkoff⁶ has given complete expressions for the nuclear Zeeman energy levels and transition frequencies appropriate to a single-crystal specimen, taking into account

* Work was performed in the Ames Laboratory of the U. S. Atomic Energy Commission. Contribution No. 1669.

¹ D. R. Torgeson and R. G. Barnes, *Phys. Rev. Letters* **9**, 255 (1962).

² R. G. Barnes, F. Borsa, S. L. Segel, and D. R. Torgeson, *Phys. Rev.* **137**, A1828 (1965).

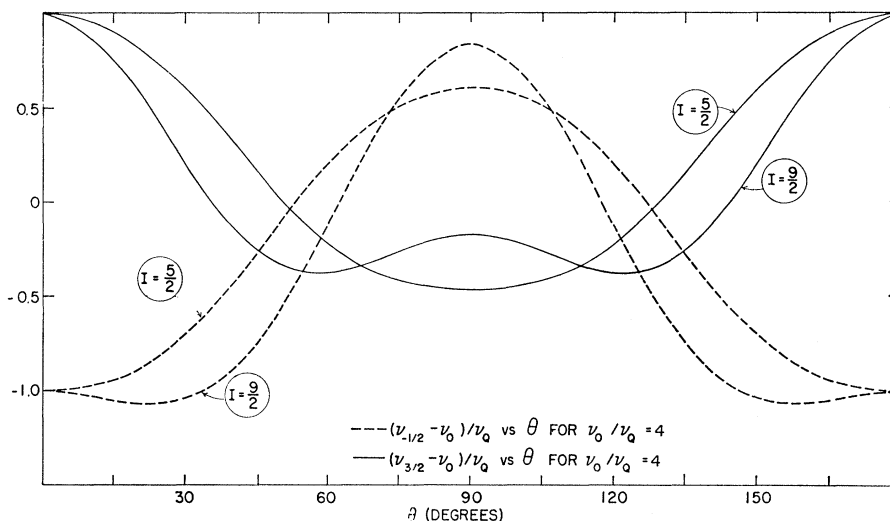
³ T. J. Rowland, in *Progress in Material Science*, edited by Bruce Chalmers (Pergamon Press, Inc., New York, 1961), Vol. 9.

⁴ W. H. Jones, Jr., and F. J. Milford, *Phys. Rev.* **125**, 1259 (1962).

⁵ R. R. Hewitt and B. F. Williams, *Phys. Rev. Letters* **12**, 216 (1964).

⁶ G. M. Volkoff, *Can. J. Phys.* **31**, 820 (1953).

FIG. 1. Comparison of the angular dependence in the single-crystal case of the resonance frequencies of the inner pair of satellite transitions for $I = \frac{5}{2}$ and $I = \frac{9}{2}$. For both spin values, the relative strength parameter $\alpha = 4$.



an electric quadrupole interaction through the third order of perturbation theory. The transition frequencies are,

$$\nu_{(m)} = \nu_0 \pm (\nu_0/\alpha)(2m-1)(E_0/eq) + (\nu_0/3\alpha^2)P_2(m) \pm (\nu_0/3\alpha^2)(2m-1)P_3(m), \quad (1)$$

where the (+) sign applies to the $m \rightarrow m-1$ transition and the (-) sign applies to the $-(m-1) \rightarrow -m$ transition, $\alpha = (\nu_0/\nu_Q) = 2I(2I-1)h\nu_0/3e^2qQ$, and $P_2(m)$ and $P_3(m)$ are given by

$$P_2(m) = c_2(m) \left| \frac{E_{\pm 2}}{eq} \right|^2 - c_1(m) \left| \frac{E_{\pm 1}}{eq} \right|^2, \quad (2)$$

$$P_3(m) = k_1(m) \left| \frac{E_{\pm 1}}{eq} \right|^2 \frac{E_0}{eq} - k_2(m) \left| \frac{E_{\pm 2}}{eq} \right|^2 \frac{E_0}{eq} - \frac{k_3(m)}{\sqrt{6}} \frac{(E_{+1})^2 E_{-2} + (E_{-1})^2 E_{+2}}{(eq)^3}. \quad (3)$$

Here, the $c(m)$ and $k(m)$ are functions of I and m ,⁶ and the E_0 , etc., have their usual definitions:

$$E_0 = (eq/4)(3 \cos^2\theta - 1), \quad (4)$$

$$E_{\pm 1} = \pm (\sqrt{6}/4)eq \sin\theta \cos\theta e^{\pm i\phi}, \quad (5)$$

$$E_{\pm 2} = (\sqrt{6}/8)eq \sin^2\theta e^{\pm 2i\phi}. \quad (6)$$

The Zeeman frequency ν_0 and lowest pure quadrupole frequency ν_Q have their customary definitions:

$$\nu_0 = \gamma H_0/2\pi, \quad (7)$$

$$\nu_Q = 3e^2qQ/2I(2I-1)h. \quad (8)$$

These expressions apply to the case of an axially symmetric field gradient tensor (FGT) characterized by the single component $eq = \partial^2 V/\partial z^2$, and the angular orientation θ of the z axis of the FGT with respect to the (external) magnetic field direction. The results are applicable to the case of a metal to the extent that the

Zeeman frequency ν_0 then includes the isotropic Knight-shift contribution to the Zeeman energy. However, these formulas do not take into account the further complications which arise from the simultaneous occurrence of Knight shift anisotropy in a noncubic metal, and which have been discussed elsewhere.⁷ In the particular case of indium, the Knight-shift anisotropy contribution to the positions of the spectrum lines is so small relative to quadrupolar effects, that this aspect can be safely neglected in a qualitative (or even semiquantitative) discussion of the spectrum. This is definitely not the case, for example, in scandium.²

The appearance of extra satellite lines in the spectrum of a powder sample may be readily understood by comparing the angular behavior of (1) for the two inner satellite lines, $m = +\frac{3}{2} \leftrightarrow +\frac{1}{2}$ and $m = -\frac{1}{2} \leftrightarrow -\frac{3}{2}$, for a fixed value of the relative strength parameter α in the cases that $I = \frac{5}{2}$ and $I = \frac{9}{2}$. Figure 1 shows this comparison for the case that $\alpha = 4$. In the $I = \frac{5}{2}$ case, the angular dependence departs only slightly from the basic $3 \cos^2\theta - 1$ dependence contributed in first order. In the $I = \frac{9}{2}$ example, however, pronounced extrema in the resonance frequency also occur at angular orientations other than 0° and 90° . Each extremum in the angular dependence of the single crystal transition corresponds to a single resonance from a powder sample (except for the extremum at 0° , there being essentially no crystallites having this orientation). Thus, each of these two transitions in the $I = \frac{9}{2}$ case yields an additional *non-90°* resonance in the powder.

Figure 1 also indicates that these *non-90°* satellite lines in the powder spectrum may appear in two locations. When the new extremum in the single crystal angular dependence appears near 90° , the new line in the powder spectrum will appear to emerge from the original 90° satellite line. On the other hand, when the new extremum first appears at zero degrees, the new line

⁷ W. H. Jones, Jr., T. P. Graham, and R. G. Barnes, Phys. Rev. **132**, 1898 (1963).

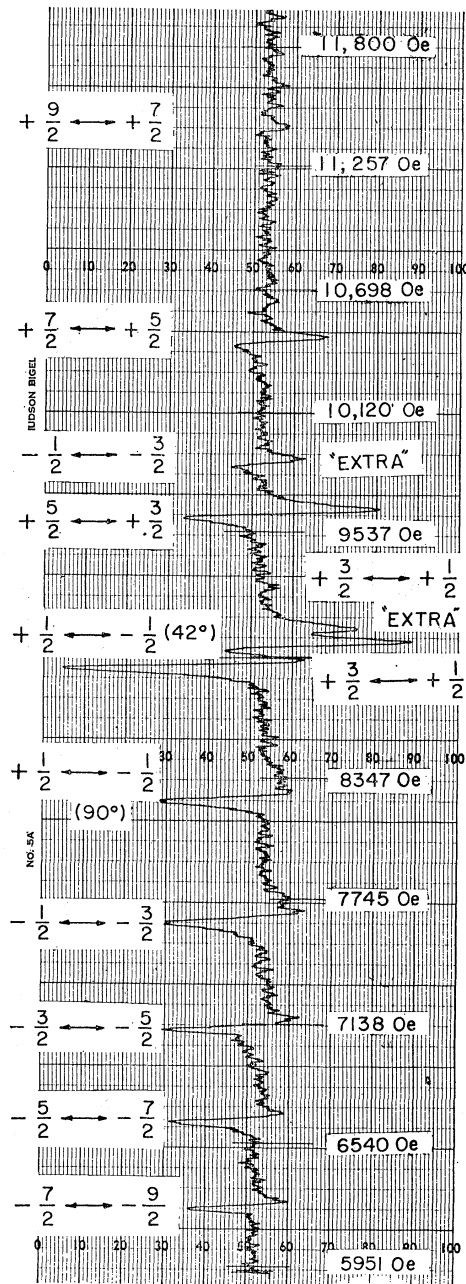


FIG. 2. Recorded example of complete spectrum of In^{115} in indium at a resonance frequency of 8.00 Mc/sec.

in the powder spectrum will first appear on the opposite side of the spectrum from the original 90° line and near the next more outwardly lying 90° satellite on that side of the spectrum.

These situations for the powder spectrum can be evaluated at least semiquantitatively by a simple extension of the usual powder specimen calculation,⁸ to

⁸ M. H. Cohen and F. Reif, in *Solid State Physics*, edited by F. Seitz and D. Turnbull (Academic Press Inc., New York, 1957), Vol. 5, p. 321.

include second-order effects for the satellite lines. The extrema in the single crystal pattern correspond to the condition⁸

$$dv(\cos\theta)/d\cos\theta=0, \quad (9)$$

and we determine the conditions under which this expression has two real roots. For the $I=\frac{9}{2}$ case, the single-crystal frequencies, through second order, of the inner satellite pair are

$$\nu(\frac{3}{2} \leftrightarrow \frac{1}{2}) - \nu_0 = \frac{1}{2}\nu_Q(3\mu^2 - 1) + (3\nu_Q^2/16\nu_0) \times (1 - \mu^2)(7 - 55\mu^2), \quad (10)$$

$$\nu(-\frac{1}{2} \leftrightarrow -\frac{3}{2}) - \nu_0 = -\frac{1}{2}\nu_Q(3\mu^2 - 1) + (3\nu_Q^2/16\nu_0) \times (1 - \mu^2)(7 - 55\mu^2), \quad (11)$$

where we have taken $\mu = \cos\theta$ for brevity. For the first of these, the condition (9) yields

$$\mu[4\alpha - (31 - 55\mu^2)] = 0. \quad (12)$$

Now, in addition to the 90° satellite line due to the root $\mu=0$ of this equation, we also have a satellite corresponding to the angular orientation $\mu' = [(31 - 4\alpha)/55]^{1/2}$, provided that $\alpha \leq 31/4$, or in other words, provided that

$$\nu_0 \leq (31/4)\nu_Q. \quad (13)$$

Thus, the new satellite line appears only in the range of Zeeman frequencies below the critical value given by (13). Since the value of μ' at this critical frequency is zero, the extra line emerges from the original 90° line and moves outward across the spectrum as the Zeeman frequency (or magnetic field) is reduced.

The other satellite line, described by (11), behaves differently. For it, the condition (9) yields

$$\mu[4\alpha + (31 - 55\mu^2)] = 0, \quad (14)$$

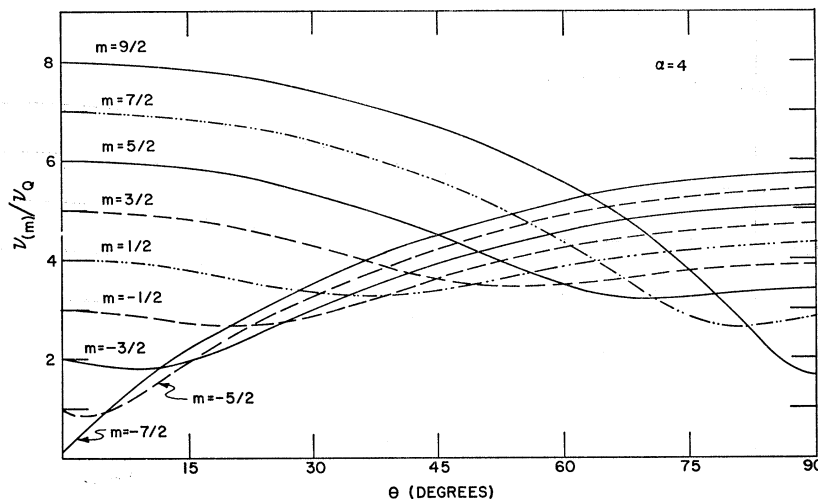
leading to a non- 90° satellite corresponding to $\mu' = [(31 + 4\alpha)/55]^{1/2}$. The critical Zeeman frequency for the appearance of this line is determined by the requirement that $(\mu')^2 \leq 1$. We have then that $\alpha \leq 6$, or that

$$\nu_0 \leq 6\nu_Q \quad (15)$$

for the allowed Zeeman frequency range. In this instance, the value of μ' at the critical frequency is unity so that the extra line appears at the $\theta=0$ position in the powder spectrum of this satellite, and moves inward across the spectrum toward its 90° mate as the Zeeman frequency is reduced.

In addition to the appearance of non- 90° satellite lines in the powder spectrum, the large quadrupole coupling causes sufficient mixing of the Zeeman states to give rise to $\Delta m = \pm 2$ transitions (in principle, $\Delta m = \pm 3$ and even more highly forbidden transitions become possible). The $\Delta m = \pm 2$ spectrum, however, consists entirely of non- 90° lines, due to the fact that the matrix elements which connect adjacent Zeeman states are proportional to $E_{\pm 1}$ (Eq. 5) and consequently vanish at $\theta=90^\circ$. Using perturbation theory, the $\Delta m = \pm 2$

FIG. 3. Calculated angular dependence of all transitions in the single-crystal case for $I = \frac{9}{2}$ and with the relative-strength parameter $\alpha = \nu_0/\nu_Q = 4$.



powder spectrum can be calculated by taking the second differences between the energy level expressions and applying the methods described above to locate the non-90° transitions and the frequency ranges within which they occur.

III. EXPERIMENTAL DETAILS

The work reported here is an extension and elaboration of the work of Torgeson and Barnes on the central transition of the In^{115} NMR spectrum in indium metal.¹ The samples used were the same as those used in that work—being dispersions of the metal in Dow-Corning silicon fluid. The same spectrum is obtained from commercial (dry) powder samples of the metal purchased from the Indium Corporation of America and from Belmont Mining and Smelting Company. In this connection it was observed that the resonances in such dry powder were only detectable in samples which had been exposed to the air sufficiently for the particles to acquire an oxide layer. Samples prepared and sealed in argon failed to show the resonance spectrum, and also gave rise to undue loading of the spectrometer rf circuitry.

A Varian Associates wide-line NMR spectrometer (induction type) was used for all measurements. The spectrometer frequency was monitored with a Computer Measurements Corp. frequency counter, and the magnetic field was measured using saturated aqueous solutions of $\text{La}^{139} \text{Cl}_3$, $\text{Al}^{27} \text{Cl}_3$, and $\text{Li}^7 \text{Cl}$, according to the field strength region. Shift measurements and results are based on the In^{115} resonance frequency in a saturated aqueous solution of InCl_3 .

In all cases the spectrum was observed by scanning the magnetic field rather than the resonance frequency. Signals of the 4.2% abundant isotope In^{113} which has a very slightly smaller magnetic moment and also a slightly smaller quadrupole moment, were not observed. In some cases, the resonance of this isotope is very likely hidden by the tails of the In^{115} resonance. An example of the complete recorded spectrum at a fre-

quency of 8.00 Mc/sec is shown in Fig. 2. A total scanning time of one-half-hour was required. In general, measurements were not made from such long scans, but rather from shorter runs over particular regions.

No special precautions were taken to insure that the sample temperature was maintained more constant than the nominal "room" temperature of 24°C. Variations of the order of $\pm 2^\circ\text{C}$ about this value do occur, and are responsible for some of the discrepancies between experimental and theoretical spectral line positions. From the known temperature dependence of the In^{115} quadrupole coupling,⁹ it follows that a 2°C temperature change will shift each of the outer satellite lines in the spectrum by 0.013 Mc/sec, the inner lines being shifted proportionately less.

IV. COMPARISON WITH THEORY—ALLOWED SPECTRUM

The experimental results are compared with the complete resonance spectrum appropriate to a powder specimen, calculated using the values of the nuclear quadrupole coupling and Knight-shift tensor components, determined from a perturbation-theory analysis of the frequency versus field dependence of the central transition of the spectrum.¹ The calculated spectrum appropriate to a powder specimen was obtained in the following manner: the energy levels of the complete Hamiltonian, including the Knight shift anisotropy.

$$\mathcal{H} = h\nu_0 I_z [1 + a(3\mu^2 - 1)] + h\nu_Q [\frac{1}{2} I_z^2 \cos^2\theta + \frac{1}{2} I_x^2 \sin^2\theta + \frac{1}{2} (I_x I_x + I_x I_z) \sin\theta \cos\theta - I(I+1)/6], \quad (16)$$

were computed numerically by diagonalization of the 10×10 matrix of this Hamiltonian for the case of $I = \frac{9}{2}$. In (16), $\nu_0 = \nu_R(1 + K_{\text{iso}})$, where $K_{\text{iso}} = +0.822 \times 10^{-2}$ is the isotropic Knight shift; and $a = K_{\text{ax}}/(1 + K_{\text{iso}}) = -0.144 \times 10^{-2}$, where K_{ax} is the axial component of

⁹ W. W. Simmons and C. P. Slichter, Phys. Rev. **121**, 1580 (1961).

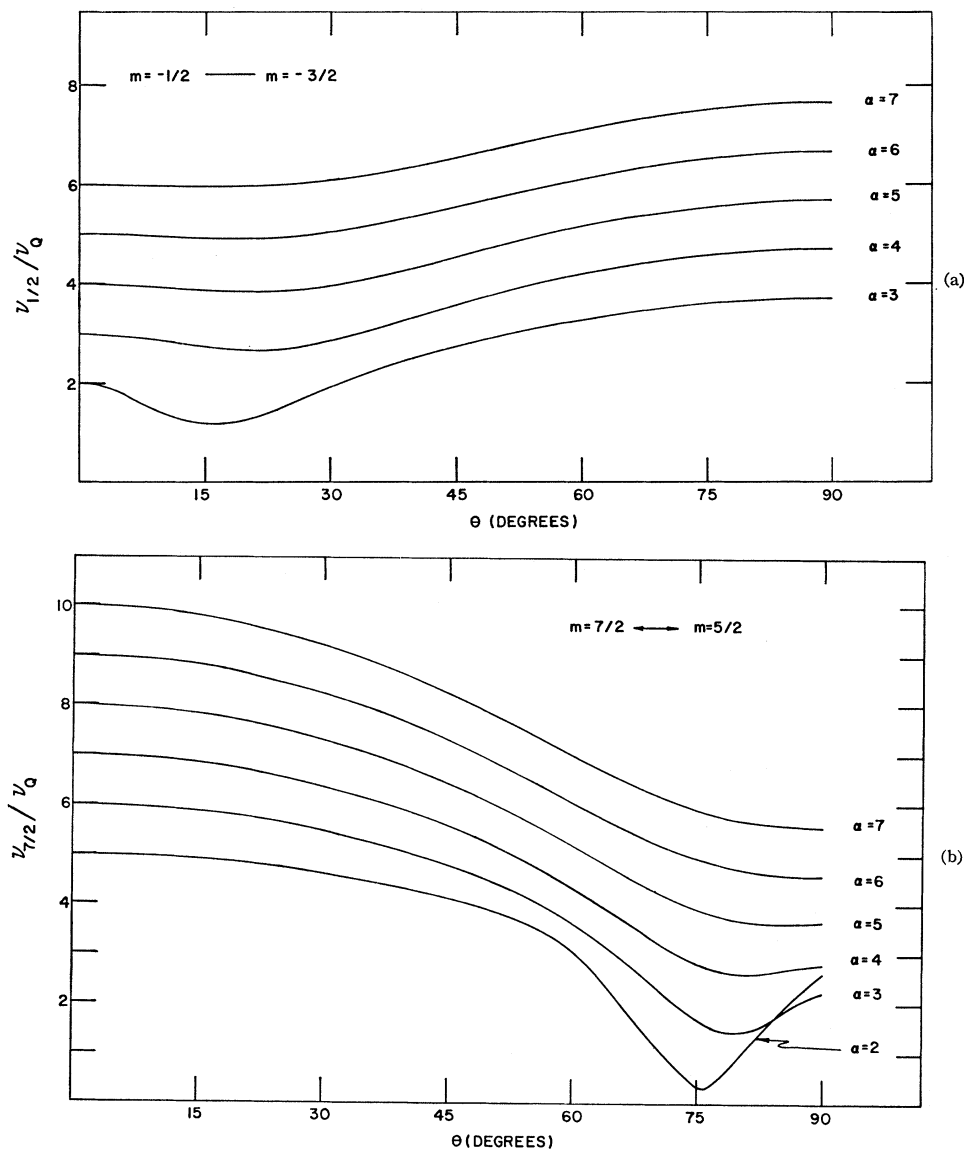


FIG. 4. (a) Angular dependence (calculated for $I = \frac{3}{2}$ of the $m = -\frac{1}{2} \leftrightarrow m = -\frac{3}{2}$ satellite line) for several values of the relative strength parameter α . The growth of the extremum in these curves in the vicinity of $\theta = 15^\circ$ corresponds to the appearance of an extra satellite line in the spectrum from a powder specimen. (b) Angular dependence (calculated for $I = \frac{3}{2}$ of the $m = \frac{7}{2} \leftrightarrow m = \frac{5}{2}$ satellite line) for several values of the relative strength parameter α . The growth of the extremum in the vicinity of 75° corresponds to the appearance of an extra satellite line in the powder-specimen spectrum.

the Knight shift tensor. ν_Q is given by (8) and was taken to be 1.2292 Mc/sec in the numerical calculations, and ν_R is the In^{115} resonance frequency in the reference solution in InCl_3 , taken with respect to the pure Zeeman states.

This calculation (i.e., the matrix diagonalization) was performed for each of 30 values of the angle θ equally spaced between 0° and 90° . The first differences of these energy eigenvalues constitute the allowed spectrum, as a function of angle, appropriate to a single-crystal specimen. As discussed above, the usual powder-specimen spectrum is that of the 90° orientation of the single crystal (except for one-half of the central transition).

In Fig. 3 we show the calculated angular dependence of the spectrum lines for the single crystal case for $\alpha = 4$, at which value most of the satellites have begun to show

secondary extrema in their angular dependence. The calculated positions of the non- 90° spectrum lines were determined by locating these secondary extrema by numerical interpolation between the machine values. Figure 4 provides an indication of the manner in which the extra satellites "grow" out of the 0° and 90° positions as the resonance frequency is decreased. The (a) portion of the figure shows this behavior for an extra line originating at the 0° position, and the (b) portion of the figure shows the situation for the extra line originating at the 90° position.

Figure 5 shows the calculated resonance frequency versus magnetic-field behavior of the allowed spectrum ($\Delta m = \pm 1$) within the frequency region determined roughly by $\alpha = 3$ to $\alpha = 13$. Both the 90° and non- 90° lines are shown.

The identification of the various lines in the spectrum

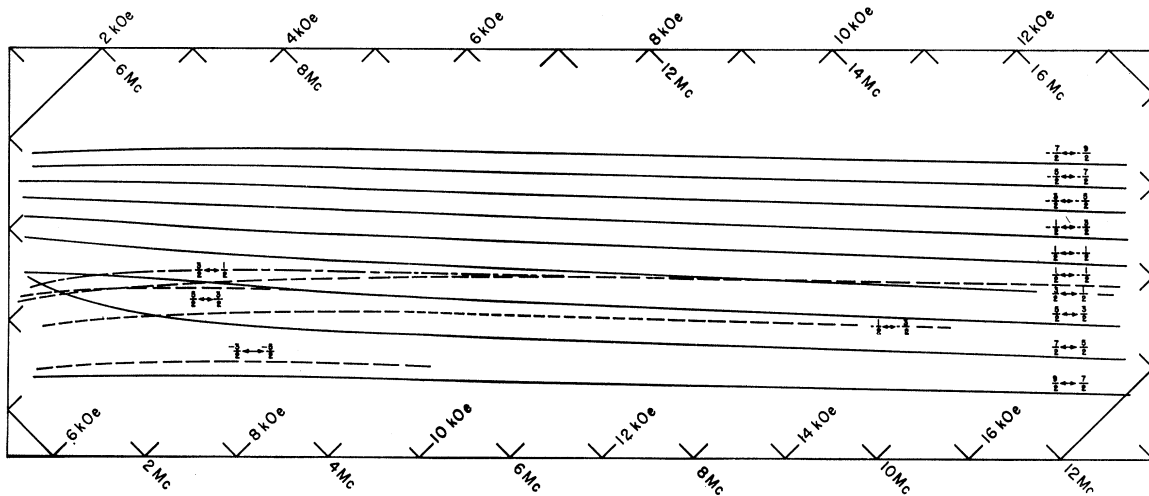


Fig. 5. Calculated frequency versus field plot of the allowed spectrum of In^{115} in indium metal. The solid lines are the usual ($\theta=90^\circ$) transitions, and the dashed lines belong to the extra (non- 90°) transitions.

of a powder specimen poses some problems. Of course, if it is possible to reach a sufficiently high frequency (field) that the splitting of the central transition is less than the spacing of the innermost satellite pair (i.e., less than ν_Q), and if all of the satellite transitions are observable, then it is a simple matter to identify the various transitions, and this is indeed a reliable and valuable check on the analysis. This situation is the one commonly encountered. However, several qualitative features of the spectrum lines do provide considerable aid in identifying the lines, and in the following we shall consider these features.

First, as is apparent in Fig. 2, the absorption derivative signals of the satellite lines characteristically point in opposite directions on opposite sides of the center of the resonance spectrum. This follows simply from the intensity distribution appropriate to a satellite in a powder-specimen spectrum.^{8,10} The same argument applies directly to the strongly split central transition, so that in the present case (indium), at a reasonably high resonance frequency (field) such that no non- 90° lines occur, the derivative spectrum consists of five lines pointing one way on one side of the center point and five lines pointing the other way on the other side.

As discussed in Sec. II the non- 90° satellite lines can originate in either of two locations in the spectrum. For the root μ' of (12), the new line emerges from the original 90° line and moves inward across the spectrum as the resonance frequency (or field) is reduced. In this case, the 90° satellite (i.e., its derivative) *reverses* its orientation while the new non- 90° satellite acquires the orientation which the 90° line originally had. This state of affairs is depicted for the $+\frac{5}{2} \leftrightarrow +\frac{3}{2}$ transitions in Fig. 6, which shows a sequence of experimental recordings at successively lower resonance frequencies. Reversal of a 90° satellite is also seen in Fig. 2 in which the

$+\frac{3}{2} \leftrightarrow +\frac{1}{2}$ transition appears split. In this case, the situation is complicated by the close proximity of the non- 90° side of the central ($+\frac{1}{2} \leftrightarrow -\frac{1}{2}$) transition.

On the other hand, the non- 90° satellite belonging to the root μ' of (14) emerges at the $\theta=0$ position, which is on the opposite side of the spectrum from its 90° mate. This non- 90° line has the same orientation as the 90° lines on *that* side of the spectrum. Thus, in both cases, the new non- 90° line has the same orientation as the 90° lines on its side of the spectrum. The appearance of a derivative signal pointing oppositely to other lines on its side of the spectrum is a clear indication that an extra line has appeared at 90° and that one of the original 90° lines has turned over.

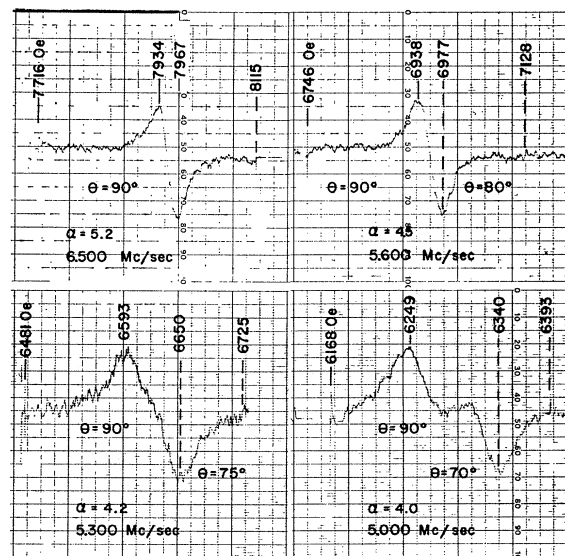


Fig. 6. Experimental behavior of the appearance of an extra satellite line in the vicinity of 90° . The transition shown is the $+\frac{5}{2} \leftrightarrow +\frac{3}{2}$, and the derivative signal of the resonance is shown.

¹⁰ F. Borsa and R. G. Barnes, J. Phys. Chem. Solids 25, 1305 (1964).

TABLE I. Comparison of predicted and observed field strengths (in kilo-oersteds) for allowed transitions in the In¹¹⁶ spectrum at several fixed resonance frequencies.

Transition	$\nu=5.000$ Mc/sec		$\nu=8.000$ Mc/sec		$\nu=14.500$ Mc/sec	
	Predicted field	Measured field	Predicted field	Measured field	Predicted field	Measured field
$+\frac{3}{2} \leftrightarrow +\frac{1}{2}$	8.270	8.288	11.238	11.364	18.360	18.338
$+\frac{1}{2} \leftrightarrow +\frac{3}{2}$	7.150	7.137	10.411	10.398	17.352	17.365
$-\frac{1}{2} \leftrightarrow -\frac{3}{2}$	6.812	6.806	9.860	9.824
(extra)						
$+\frac{3}{2} \leftrightarrow +\frac{1}{2}$	6.310	6.335
(extra)						
$+\frac{1}{2} \leftrightarrow +\frac{3}{2}$	6.245	6.223	9.590	9.583	16.602	16.615
$+\frac{3}{2} \leftrightarrow +\frac{1}{2}$	6.128	6.118	9.042	9.013	15.730	15.708
(42°)						
$+\frac{3}{2} \leftrightarrow +\frac{1}{2}$	5.954	5.940	8.970	8.956
(extra)						
$+\frac{1}{2} \leftrightarrow +\frac{3}{2}$	5.510	5.489	8.862	8.822	15.900	15.907
$+\frac{3}{2} \leftrightarrow +\frac{1}{2}$	4.910	4.922	8.211	8.180	15.235	15.235
(90°)						
$-\frac{1}{2} \leftrightarrow -\frac{3}{2}$	4.400	4.376	7.636	7.605	14.616	14.605
$-\frac{3}{2} \leftrightarrow -\frac{1}{2}$	3.960	3.935	7.114	7.086	14.040	14.028
$-\frac{1}{2} \leftrightarrow -\frac{3}{2}$	3.590	3.560	6.646	6.620	13.488	13.478
$-\frac{3}{2} \leftrightarrow -\frac{1}{2}$	3.265	3.235	6.228	6.198	12.970	12.966

An extra satellite line which originates at $\theta=0$ (e.g., in the $-\frac{1}{2} \leftrightarrow -\frac{3}{2}$ transition in the indium spectrum) possesses an additional curious feature. According to (15), the allowed Zeeman frequency range for this extra satellite is $\nu_0 \leq 6\nu_Q$. However, this inequality is based on the appearance of an actual infinity in the function $|d\nu/d\mu|^{-1}$, or in other words, to the appearance of a root in $d\nu/d\mu$. But as is known to be the case for the central transition of the spectrum when both quadrupolar and anisotropic shift effects are present,⁷ there exists an intermediate region of frequency within which the singularity at $\theta=0$ changes smoothly from an infinity to a step of finite height. An approximate idea of the extent of this region may be obtained by deter-

mining the highest resonance frequency at which $d^2\nu/d\mu^2$ evaluated at $\theta=0$ ($\mu=1$) vanishes:

$$[d^2\nu(-\frac{1}{2} \leftrightarrow -\frac{3}{2})/d\mu^2]_{\mu=1} = 0. \tag{17}$$

Using (11), we obtain

$$[(165\mu^2 - 31) - 4\alpha]_{\mu=1} = 0, \tag{18}$$

which yields $\alpha=67/2$. Thus, within the region $6\nu_Q \leq \nu_0 \leq 33\nu_Q$ we can expect that this extra satellite line will continue to exhibit some intensity—strongest of course near $\nu_0=6\nu_Q$. Figure 7 shows this behavior for the $\theta=0$ resonance of the $-\frac{1}{2} \leftrightarrow -\frac{3}{2}$ transition in indium, which occurs very close to the $\theta=90^\circ$ resonance of the $+\frac{5}{2} \leftrightarrow +\frac{3}{2}$ transition. This same line is also clearly discernible in Fig. 2.

It is not feasible to present a meaningful comparison of the experimental and theoretical spectra on a plot which would occupy a single page. During the course of this investigation, it was found convenient to work with a plot about 8×8 ft which was mounted on a wall of the laboratory. To give an indication of the agreement of the results, however, we have listed in Table I the calculated and measured field strengths of the allowed 90° lines and the two halves of the central transition for a number of fixed resonance frequencies. Inasmuch as the calculations are made for fixed field strengths, the tabulated resonance fields for fixed frequency are obtained by interpolation. The calculations were made at intervals of $\alpha=1$, corresponding to magnetic field intervals of 1307.4 Oe.

V. COMPARISON WITH THEORY—FORBIDDEN SPECTRUM

As pointed out in Sec. II, the large quadrupole coupling causes sufficient mixing of the Zeeman levels to give rise to observable $\Delta m = \pm 2$ transitions. These

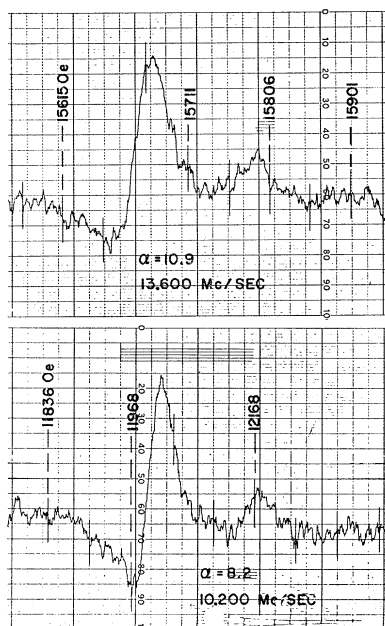


FIG. 7. Experimental behavior of the appearance of an extra satellite line in the vicinity of 0°. The transition shown is the $-\frac{1}{2} \leftrightarrow -\frac{3}{2}$, and the derivative signal of the resonance is shown.

transitions all have vanishing intensity at $\theta=90^\circ$, because then the $\Delta m=\pm 1$ matrix elements of (16), which are proportional to $E_{\pm 1}$ (Eq. 5), vanish. Consequently, the observable $\Delta m=\pm 2$ transitions occur only at angles other than 90° . Calculated frequency versus field curves for these forbidden lines were obtained by taking the second differences of the energy eigenvalues of (16), as a function of angular orientation. As in the case of the allowed spectrum, the extrema in these curves were located by numerical interpolation. Because the $\Delta m=\pm 2$ lines are all non- 90° transitions, they occur mainly at relatively low resonance frequencies (small α). The intensity of these lines is, of course, also greatest at small α values. The behavior of those lines which occur within the span of the allowed spectrum is depicted in Fig. 8 which also shows the allowed transitions in the same region.

VI. LINE SHAPES AND WIDTHS

As is customary, the static dipolar broadening terms have not been included in the Hamiltonian (16). The effect of these interactions is considered by weighting the frequency-distribution envelope of the individual transition with a line-shape function appropriate to the resonance contribution from a single crystallite.^{10,11} Simmons and Slichter⁹ found the shape of the In¹¹⁵ pure quadrupole resonance lines to be very closely approximated by a Gaussian curve, and we obtain a similar result. Since the function used to describe the frequency distribution envelope of a particular transition is obtained from perturbation theory, and can therefore become quite complicated in the present case, we have compared the experimental and calculated line shapes at a sufficiently high Zeeman frequency that second and higher order terms in the frequency dependence are negligible. Under these conditions the frequency distribution function for an individual satellite transition is identical with that appropriate to the case of broadening by an axially symmetric anisotropic Knight shift.⁷ The latter problem has been treated recently by Rowland and Hughes¹¹ and also by Borsa and Barnes.¹⁰

Comparison of the calculated and observed line shapes for three satellite transitions is shown in Fig. 9. The synthetic line shapes were calculated in the manner described in Ref. 10, using a Gaussian shape function for the single-crystal resonance. A full width at half-maximum intensity of 40 kc/sec for this Gaussian shape is found to give satisfactory fit for all three satellites. This value (40 kc/sec) compares quite well with the full widths obtained by Simmons and Slichter for their sample B,⁹ but is somewhat larger than the widths reported by Hewitt and Taylor.^{11a} More quantitative comparison of the satellite widths would require that the

theory of the dipolar broadening of the satellite transitions for arbitrary half-integral spin be worked out.

We have also compared the observed central transition of the spectrum with synthetic shapes calculated as in the case of the satellites, but using the second-order perturbation-theory expression for the frequency distribution function which includes the effects of both quadrupole and anisotropic Knight-shift interactions.⁷ In this case, the best fit of the synthetic line shape to that observed is obtained with a full width at half-maximum intensity of 48 kc/sec for the Gaussian weighting function. The dipolar second moment for the central transition can be calculated from the formula given by Kambe and Ollom,¹² in the form appropriate to a powder specimen:

$$\langle H_z^2 \rangle_{Av} = (9/5) F_L(I) \gamma^2 \hbar^2 \sum_k r_{jk}^{-6}. \quad (19)$$

$F_L(I)$ is a complicated function of I which has the value 1961/180 in the present case ($I=\frac{9}{2}$). At room temperature, we obtain for the lattice summation, $\sum_k r_{jk}^{-6} = 12.26a_0^{-6}$, taking account of the 200 nearest neighbors. Here, a_0 is the basal-plane cell edge of the body-centered tetragonal cell ($a_0=3.2408 \text{ \AA}$ and $c/a_0=1.5233$). We then have from (19) that $\langle H_z^2 \rangle_{Av} = 5.05 \text{ Oe}^2$, leading to a Gaussian width of 4.50 Oe, which differs little from the value obtained (4.76 Oe) assuming the lattice to be face-centered cubic. This result simply confirms the fact that, considered from the standpoint of close packing, the indium lattice departs only slightly from cubic symmetry. The calculated nuclear dipolar width is therefore roughly an order-of-magnitude too small, the excess width presumably arising from some sort of indirect exchange interaction.⁹

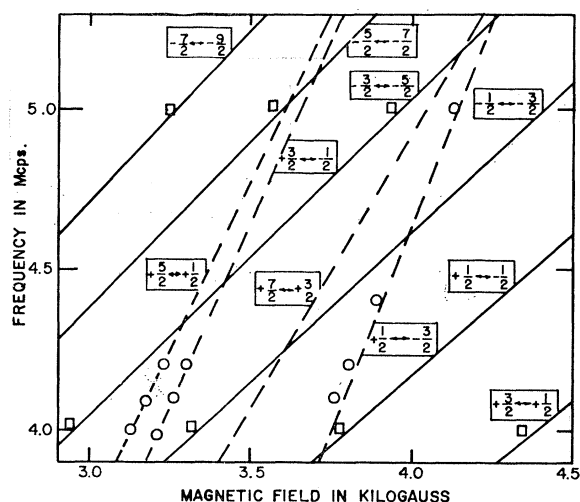
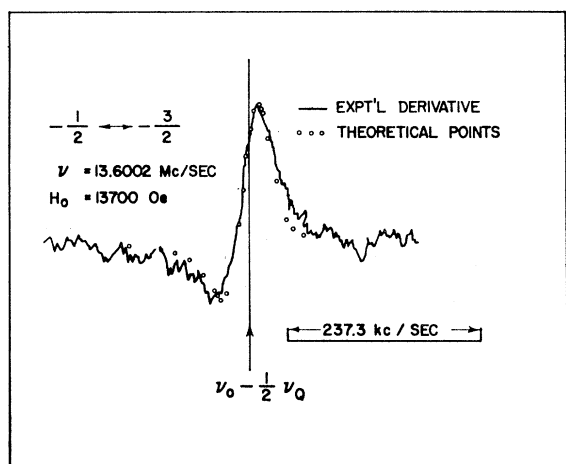


Fig. 8. Lines of the "forbidden" $\Delta m=\pm 2$ spectrum of In¹¹⁵ in indium powder. The dashed lines are the calculated positions of the forbidden resonances, and the solid lines are those of the allowed ($\Delta m=\pm 1$) transitions occurring in the same region. The circles show the observed forbidden lines and the squares the observed allowed lines.

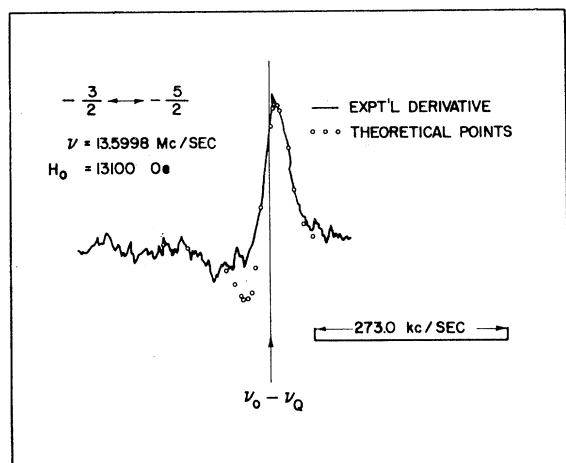
¹¹ D. G. Hughes and T. J. Rowland, Can. J. Phys. **42**, 209 (1964).

^{11a} R. R. Hewitt and T. T. Taylor, Phys. Rev. **125**, 524 (1962).

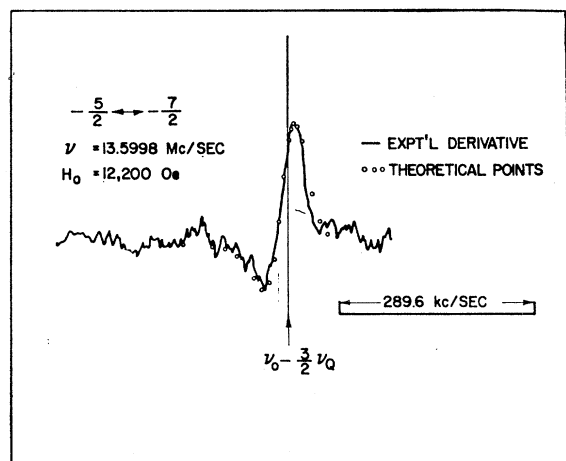
¹² K. Kambe and J. F. Ollom, J. Phys. Soc. Japan **11**, 50 (1956).



(a)



(b)



(c)

FIG. 9. Experimental traces of the first three satellite lines on the high-frequency (low-field) side of the spectrum, taken at a fixed frequency of 13.60 Mc/sec. The theoretical points shown by circles are obtained from synthetic line shapes calculated using a Gaussian-shape function for the single-crystal resonance with a full width of 40 kc/sec.

No differences were observed in the shapes or widths of the resonances obtained with the various samples of indium metal (see also Sec. III). Both the dry powders and the oil dispersion yielded the same results.

VII. DISCUSSION

The fact that the complete NMR spectrum of In^{115} in the powdered metal is observed with such strong intensity corroborates several arguments respecting the anticipated NMR spectra of nuclei which experience large quadrupole couplings:

(a) The magnitude of the quadrupole coupling, e^2qQ/h , is not the relevant quantity to consider in estimating the importance of quadrupole effects on the Zeeman levels. Rather, as first pointed out by Volkoff,⁶ the lowest pure quadrupole frequency, ν_Q , is the quantity that must be compared with the Zeeman frequency, ν_0 , in order to estimate the importance of quadrupole effects. Thus, for example, in the case of gallium metal in which the pure quadrupole frequencies of Ga^{69} and Ga^{71} have been observed,¹³ the quadrupole couplings of these nuclei are smaller than that of In^{115} in indium. Yet, because the spins of the gallium isotopes are $\frac{3}{2}$, the factor ν_Q is significantly larger for both of these isotopes than for In^{115} in indium. The result is that the condition $\alpha=1$ requires a field strength of 10.6 kOe for Ga^{69} and 5.3 kOe for Ga^{71} in gallium, whereas for In^{115} , $\alpha=1$ at 1.307 kOe in indium. The indium example is therefore more amenable to typical NMR spectrometers and laboratory magnets than is the gallium case.

(b) The extent to which the NMR spectrum is "smeared out" is a reflection of the degree of field gradient inhomogeneity rather than of the strength of the quadrupole interaction as such. In the case of indium, the field gradient appears to be remarkably homogeneous, very likely because the metal is readily obtainable in high purity and because its low melting point insures that lattice strains anneal at or near room temperature. In other cases, e.g., scandium and lanthanum^{2,14,15} it is very difficult to observe all of the satellite transitions even though both the quadrupole coupling and ν_Q are smaller than for In^{115} in indium. The failure thus far to detect NMR in a number of hexagonal metals (Ti, Zr, Hf) is very likely due to field gradient inhomogeneity. A more quantitative discussion of the role of field-gradient inhomogeneities in determining the appearance of NMR spectra will be presented elsewhere.¹⁵

The values of the Knight-shift components, K_{iso} and K_{ax} , and of the In^{115} quadrupole coupling used as the basis of the calculation of the energy levels and transition frequencies were those obtained previously from a

¹³ W. Knight, Phys. Rev. **104**, 271 (1956).

¹⁴ D. R. Torgeson and R. G. Barnes, Phys. Rev. **136**, A738 (1964).

¹⁵ B. R. McCart and R. G. Barnes (to be published).

perturbation-theory analysis of the central transition data alone.¹ The generally excellent agreement obtained between measured and calculated resonance field strengths for the complete spectrum (Table I) confirms the appropriateness of the perturbation analysis for determining the interaction parameters.

In this respect, it would be most interesting to determine the temperature dependence of the Knight-shift components. In particular, the strong temperature dependence of the quadrupole coupling in indium, which is not accounted for by the lattice contribution to the field gradient, suggests that K_{ax} may possess a rather strong temperature dependence. Perturbation-theory analysis of central-transition data should suffice for the

determination of K_{ax} and K_{iso} . A first step in this direction, taken by Hewitt *et al.*,¹⁶ indicates that K_{iso} at 4.2°K differs very little from the room-temperature result.

ACKNOWLEDGMENTS

The authors are indebted to W. J. Haas for making available his computer program for matrix diagonalization and for considerable assistance with the computer programming, and to Dr. F. Borsa for the calculation of the satellite line shapes.

¹⁶ R. R. Hewitt, J. E. Adams, Jr., and L. Berry, *Bull. Am. Phys. Soc.* **9**, 732 (1964).

Spin-Lattice Relaxation in Some Rare-Earth Salts. II. Angular Dependence, Hyperfine Effects, and Cross Relaxation*

G. H. LARSON† AND C. D. JEFFRIES‡

Department of Physics, University of California, Berkeley, California

(Received 3 December 1965)

In this second part of a study of the spin-lattice relaxation rate T_1^{-1} in the temperature range $1.2 \leq T \leq 5^\circ\text{K}$ of some trivalent rare-earth ions in the salts $\text{La}_2\text{Mg}_3(\text{NO}_3)_{12} \cdot 24\text{H}_2\text{O}[\text{LaMN}]$, $\text{La}(\text{C}_2\text{H}_5\text{SO}_4)_3 \cdot 9\text{H}_2\text{O}[\text{LaES}]$, and $\text{Y}(\text{C}_2\text{H}_5\text{SO}_4)_3 \cdot 9\text{H}_2\text{O}[\text{YES}]$, we examine the dependence of T_1^{-1} on the angle θ between the crystal symmetry axis and the magnetic field \mathbf{H} . Data are obtained from the transient recovery of the microwave paramagnetic resonance at $\nu \approx 9$ Gc/sec for Nd:YES, Nd:LaES, Nd:LaMN, Sm:LaMN, Sm:LaES, Sm:YES, Er:LaES, and Er:YES, all for isotopes of spin $I=0$. There is a decided anisotropy of the direct process, as large as 15:1, which seems to be moderately well explained by the same simple theoretical procedure used in part I for the temperature dependence. The Raman process was found to be independent of θ and H , as expected theoretically; likewise for the Orbach process, except for Nd:LaMN, where a small anisotropy is observed and explained. The data for the phonon-bottlenecked cases Ce:LaMN and Pr:LaMN indicate that the spins interact only with the phonons within the paramagnetic-resonance linewidth. The direct process for the various hyperfine lines of Er^{167} in Er:YES and Nd^{148} in Nd:LaMN is measured and found to exhibit a dependence on M_I and H in accordance with the theory of Baker and Ford, showing the importance of "forbidden" relaxation transitions $\Delta M_S = 1$, $\Delta M_I = \pm 1$. In a study of relaxation in (Er, Ce):LaES we find that the Er relaxation rate is quite well explained in its dependence on both temperature and Ce concentration by resonance cross relaxation with Ce ions in the excited state at $\Delta = 5.7^\circ\text{K}$.

I. INTRODUCTION

IN the first part of these studies,¹ which we refer to as I, we reported detailed measurements of the dependence on temperature T in the liquid-helium region of the spin-lattice relaxation processes of several paramagnetic rare-earth ions diluted in the diamagnetic host crystals lanthanum magnesium nitrate $\text{La}_2\text{Mg}_3(\text{NO}_3)_{12} \cdot 24\text{H}_2\text{O}$ (LaMN), lanthanum ethyl sulfate $\text{La}(\text{C}_2\text{H}_5\text{SO}_4)_3 \cdot 9\text{H}_2\text{O}$ (LaES), and yttrium ethyl sulfate $\text{Y}(\text{C}_2\text{H}_5\text{SO}_4)_3 \cdot 9\text{H}_2\text{O}$ (YES). These studies, together

with the earlier paper of Scott and Jeffries,² referred to as S&J, have shown that the relaxation rates have the expected temperature dependences $T_{1d}^{-1} \propto T$, $T_{10}^{-1} \propto e^{-\Delta/T}$, and $T_{1R}^{-1} \propto T^7$ or T^9 for the direct, Orbach, and Raman processes, respectively. Furthermore the magnitudes are found to be in moderate agreement with our calculations based on Orbach's³ phenomenological treatment, which assumes that the dominant interaction is that of Van Vleck,⁴ Kronig,⁵ and Fierz⁶: interaction of the orbital wave functions with the thermally modulated crystalline electric fields, together with spin-orbit interaction. Similar studies by other workers, referred to in I, confirm this.

* Supported in part by the U. S. Atomic Energy Commission.

† Present address: Central Research Department, Experimental Station, E. I. du Pont de Nemours and Company, Wilmington, Delaware.

‡ NSF Fellow, 1965-'66, in Division of Applied Physics, Pierce Hall, Harvard University, Cambridge, Massachusetts.

¹ G. H. Larson and C. D. Jeffries, *Phys. Rev.* **141**, 461 (1966).

² P. L. Scott and C. D. Jeffries, *Phys. Rev.* **127**, 32 (1962).

³ R. Orbach, *Proc. Roy. Soc. (London)* **A264**, 458 (1961).

⁴ J. H. Van Vleck, *Phys. Rev.* **57**, 426 (1940).

⁵ R. de L. Kronig, *Physica* **6**, 33 (1939).

⁶ M. Fierz, *Physica* **5**, 433 (1938).